Water Splitting

Deutsche Ausgabe: DOI: 10.1002/ange.201506294
Internationale Ausgabe: DOI: 10.1002/anie.201506294

The Interaction of Water with Free $Mn_4O_4^+$ Clusters: Deprotonation and Adsorption-Induced Structural Transformations

Sandra M. Lang, Thorsten M. Bernhardt, Denis M. Kiawi, Joost M. Bakker,* Robert N. Barnett, and Uzi Landman**

Abstract: *As the biological activation and oxidation of water takes place at an inorganic cluster of the stoichiometry $CaMn_4O_5$, manganese oxide is one of the materials of choice in the quest for versatile, earth-abundant water splitting catalysts. To probe basic concepts and aid the design of artificial water-splitting molecular catalysts, a hierarchical modeling strategy was employed that explores clusters of increasing complexity, starting from the tetramanganese oxide cluster $Mn_4O_4^+$ as a molecular model system for catalyzed water activation. First-principles calculations in conjunction with IR spectroscopy provide fundamental insight into the interaction of water with $Mn_4O_4^+$, one water molecule at a time. All of the investigated complexes $Mn_4O_4(H_2O)_n^+$ ($n = 1$–7) contain deprotonated water with a maximum of four dissociatively bound water molecules, and they exhibit structural fluxionality upon water adsorption, inducing dimensional and structural transformations of the cluster core.*

The endeavor to develop earth-abundant materials for efficient catalytic water splitting is an outstanding challenge in current catalysis research. In nature, the dissociation and oxidation of water is catalyzed by an inorganic $CaMn_4O_5$ cluster, which together with its protein ligands forms the oxygen evolving complex (OEC) of photosystem II. This biological catalyst has inspired the preparation of functional synthetic analogues of the OEC containing bi- and tetranuclear manganese oxide complexes.[1] Furthermore, solid manganese oxide and calcium–manganese oxide materials have been used as biomimetic water splitting catalysts.[1e,2]

To aid the design of artificial water splitting catalysts, we have embarked on a research program where deconvolution of the mechanisms and functionalities of the OEC is approached through hierarchical modeling, starting from $Mn_4O_4^+$ and increasing the complexity of the model system in a staged controlled manner. Studies of the reaction of $Mn_4O_4^+$ with $D_2{}^{16}O$ and $H_2{}^{18}O$ in a gas-phase ion trap apparatus revealed, along with the fast adsorption of multiple water molecules, facile exchange of the oxygen atoms of the cluster with water oxygen atoms.[3] This provided direct experimental evidence for the ability of $Mn_4O_4^+$ to deprotonate water by hydroxylation of the oxo bridges of the cluster.

Concurrent first-principles calculations offered new fundamental views on the mechanism of water binding and dissociation on the tetramanganese oxide cluster ion.[3] In particular, a two-dimensional (2D) ring-like ground state structure was found for the bare $Mn_4O_4^+$ cluster while a cuboidal isomer was found to be 24 kJ mol^{-1} higher in energy (see Figure 1, structures A and B; further higher energy isomeric structures are given in the Supporting Information, Figure S1). However, molecular adsorption of at least two water molecules has been predicted to induce a dimensionality change of the $Mn_4O_4^+$ cluster core (Figure 1, structures C–F).[3a] The resulting three-dimensional (3D) cuboid comprises μ_3-bridging oxygen atoms similar to the structure of the inorganic core of the OEC[4] with the H_2O molecules bound to the Mn atom vertices via the oxygen atom. Furthermore, using the example of $Mn_4O_4(H_2O)_4^+$ it

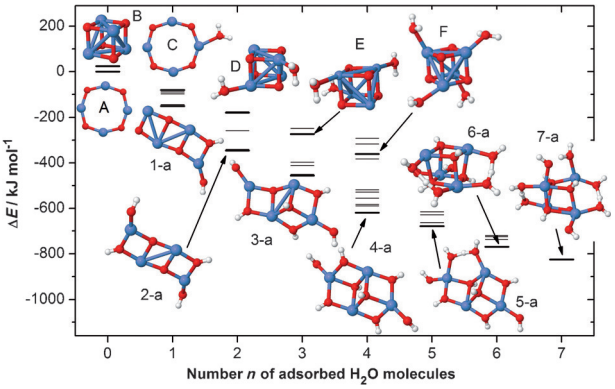

Figure 1. Calculated binding energies of n water molecules to $Mn_4O_4^+$ for different isomeric structures (denoted as energy difference ΔE with respect to the bare $Mn_4O_4^+$ cluster in the geometry A). For energies represented by bold lines, the geometric structures are shown: complexes containing only molecularly bound water (C–F) and the global minimum energy structures identified in the theoretical simulations (1-a to 7-a). Mn purple, O red, H white.

[*] Dr. S. M. Lang, Prof. Dr. T. M. Bernhardt
Institute of Surface Chemistry and Catalysis, University of Ulm
Albert-Einstein-Allee 47, 89069 Ulm (Germany)
E-mail: sandra.lang@uni-ulm.de
D. M. Kiawi, Dr. J. M. Bakker
Radboud University
Institute for Molecules and Materials, FELIX Laboratory
Toernooiveld 7, 6525 ED Nijmegen (The Netherlands)
E-mail: j.bakker@science.ru.nl
D. M. Kiawi
Anton Pannekoek Institute, University of Amsterdam
Science Park 904, 1098 XH Amsterdam (The Netherlands)
Dr. R. N. Barnett, Prof. Dr. U. Landman
School of Physics, Georgia Institute of Technology
Atlanta, Georgia 30332-0430 (United States)
E-mail: uzi.landman@physics.gatech.edu

Supporting information for this article is available on the WWW under http://dx.doi.org/10.1002/anie.201506294.

has been demonstrated that this dimensionality crossover significantly facilitates the subsequent water deprotonation reaction, manifested in: 1) lower barriers for activation of the water O–H bonds, and 2) a considerably more exothermic hydrogen migration to the μ-oxo bridges for the 3D cuboid compared to the 2D ring-like isomer.[3a]

Here we have engaged in a systematic investigation of a series of $Mn_4O_4(H_2O)_n^+$ ($n=1$–7) complexes, with the use of first-principles calculations (see the Supporting Information) in conjunction with infrared multiple-photon dissociation (IR-MPD) spectroscopy, to uncover changes in the cluster structure with each adsorbed water molecule. The structures of water clusters[5] and the reactions of water with transition-metal and metal oxide clusters were studied previously,[6] whereas this is the first study of the interaction of water with metal oxide clusters using vibrational spectroscopy.

Figure 1 shows spin density functional theory (SDFT)-calculated[7] binding energies, and the geometric structures of the lowest energy isomers of $Mn_4O_4(H_2O)_{1-7}^+$ (labeled 1-a to 7-a, with further isomeric structures given in Figure 3 and the Supporting Information, Figures S2–S8). Most interestingly, each minimum energy structure contains deprotonated water; that is, the dissociation of water is exothermic for all $Mn_4O_4^+$–water complexes. The dissociation of water occurs by hydroxylation of the cluster μ-oxo-bridges, which consequently limits the number of dissociated water molecules to a maximum of four. Thus, the predicted minimum energy structures of $Mn_4O_4(H_2O)_n^+$ ($n=5$–7) contain four dissociatively and ($n-4$) molecularly adsorbed H_2O molecules. These intact water molecules each bind to a Mn atom by the oxygen atom as well as to a neighboring OH group via a hydrogen bond to form an H_3O_2 group.

Furthermore, the dissociative adsorption of a progressively larger number of water molecules entails a structural change of the $Mn_4O_4^+$ cluster core. Dissociative adsorption of merely one H_2O molecule already induces a structural transition from the ring-like geometry of the bare cluster (structure A) to a ladder-like structure (1-a). Dissociative adsorption of a third water molecule results in a three-dimensional cluster core comprising an open cube Mn_3O_4 unit (with one vertex missing) and the fourth Mn atom coordinated to the open cube via one of the corner oxygen atoms and an additional oxygen atom (structure 3-a). This structural motif is retained for the adsorption of a total of five water molecules. Upon adsorption of a sixth H_2O a final structural change to a cuboidal geometry (structure 6-a) is observed which represents the minimum energy geometry for all larger water complexes.

In complementary IR-MPD spectroscopic experiments, we have further explored the deprotonation of the sequentially adsorbed water molecules and the structural transformations of the $Mn_4O_4^+$core. Figure 2 displays the dissociation spectra recorded on mass signals corresponding to the different water complexes $Mn_4O_4(H_2O)_n^+$ ($n=1$–7), that is, the change of the mass peak intensity ratio I/I_0 upon laser irradiation as a function of the spectral wavenumber, where I and I_0 represent the intensities with and without laser light, respectively. If the light is not resonant with a vibrational transition of the respective cluster, no fragmentation ensues

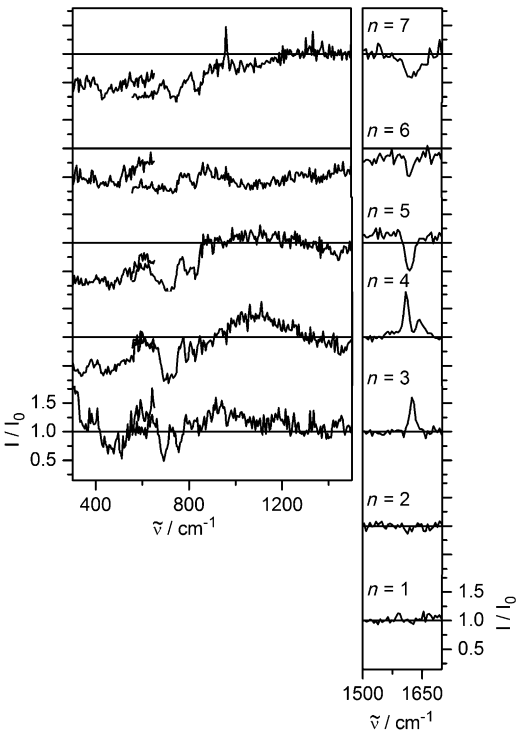

Figure 2. Experimental IR-MPD spectra of the hydrated clusters $Mn_4O_4(H_2O)_n^+$, showing the mass signal intensity ratio with and without laser light I/I_0 as a function of the laser wavenumber $\tilde{\nu}$.

and the ratio is 1. Resonant absorption of IR photons leads to fragmentation of the complex which results in $I/I_0<1$ and a "depletion" in the IR-MPD spectrum. Conversely, I/I_0 values larger than 1 ("gain") indicate that the current mass represents a fragmentation product of larger $Mn_xO_y(H_2O)_m^+$ ($m>n$ or $x,y>4$) clusters which are present in the experiment at the same time.

The most characteristic vibration in the studied spectral region is the HOH bending mode of molecularly bound water at 1550–1700 cm^{-1} (depending on the exact adsorption geometry). For the three smallest water complexes $Mn_4O_4(H_2O)_{1-3}^+$ no depletion ($I/I_0<1$) signals are detected in the HOH bending mode region. This demonstrates that the first three water molecules are deprotonated, that is, they adsorb dissociatively on the cluster, which is in full agreement with the predicted minimum energy structures of these complexes.

In marked contrast, all larger water complexes $Mn_4O_4(H_2O)_n^+$ ($n=4$–7) exhibit activity in the spectral region characteristic for the HOH bending vibration, indicating that intact water molecules are bound to these clusters. In the case of $Mn_4O_4(H_2O)_4^+$, a double peak structure is detected at 1590–1680 cm^{-1}. This structure is caused by a broad gain (that is, buildup of the tetra-water $Mn_4O_4^+$ mass signal in the above spectral range) owing to the fragmentation of $Mn_4O_4(H_2O)_5^+$ by loss of H_2O, overlapping with a depletion signal, manifested as a notch (dip) in the gain signal owing to resonant fragmentation of the $Mn_4O_4(H_2O)_4^+$ complex at a center wavenumber of 1624 cm^{-1}. This depletion of $Mn_4O_4(H_2O)_4^+$ by loss of H_2O at 1624 cm^{-1} is mirrored by the observed gain signal for $Mn_4O_4(H_2O)_3^+$. Underlying the aforementioned

depletion is the bending mode of the intact water molecule in the first structural isomer (marked −590 kJ mol^{-1} in the Supporting Information, Figure S5) of the tetra-hydrated $Mn_4O_4^+$ cluster, which lies 30 kJ mol^{-1} higher in energy with reference to the fully-deprotonated ground state structure of $Mn_4O_4(H_2O)_4^+$ (see 4-a in Figure 1); the accurate ordering of the structural isomers of the tetraoxide manganese clusters has been checked with the inclusion of van der Waals interactions in the DFT calculations (see the Supporting Information).

For all larger clusters $Mn_4O_4(H_2O)_{5-7}^+$ the observed spectral depletion features at 1619–1625 cm^{-1} are consistent with the theoretically predicted minimum energy structures containing at least one molecularly adsorbed H_2O. The band center of the HOH bending mode shifts from 1619 cm^{-1} for $Mn_4O_4(H_2O)_5^+$ and $Mn_4O_4(H_2O)_6^+$ to 1625 cm^{-1} for $Mn_4O_4(H_2O)_7^+$ while the signal width broadens from a full width at half maximum (FWHM) of 24 cm^{-1} for $Mn_4O_4(H_2O)_5^+$ to 58 cm^{-1} for $Mn_4O_4(H_2O)_7^+$. This signal broadening could be caused by subtle differences in the binding of the H_2O molecules and/or the presence of different isomers.

At wavenumbers below 1500 cm^{-1} the spectra of the complexes $Mn_4O_4(H_2O)_{3-7}^+$ exhibit clear features as well. In particular, we observe a broad depletion band below 600 cm^{-1} and several more discrete bands above 600 cm^{-1}. These bands broaden with increasing number of water molecules in the cluster complex, which might again indicate the presence of several isomeric structures that contribute to the observed signals.

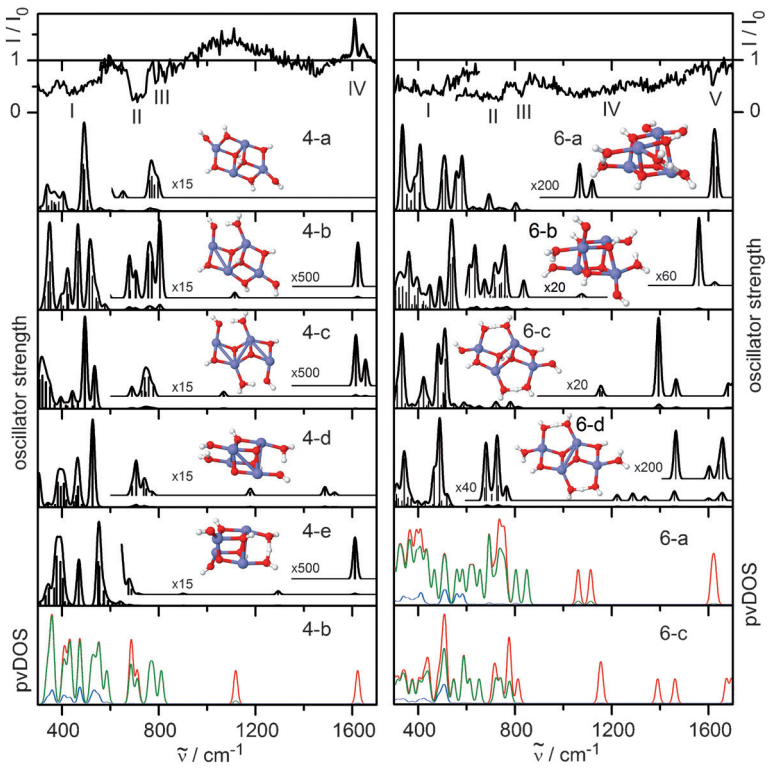

Figure 3. IR-MPD spectra (top) and calculated vibrational spectra of different isomeric structures of $Mn_4O_4(H_2O)_4^+$ (left column) and $Mn_4O_4(H_2O)_6^+$ (right column). The calculated spectra (sticks) are convoluted with a Gaussian line shape function with a FWHM of 20 cm^{-1}. Also shown are the projected vibrational density of states (pvDOS, per cm^{-1}) for isomers 4-b, 6-a, and 6-c. The red curves represent the total vDOS while the green and blue curves represent the projections on O/OH and Mn, respectively (see Theoretical Methods section in the Supporting Information). In the structural models: Mn purple, O red, H white.

For a more detailed discussion of this range of the IR-MPD spectra, we will focus in the following on two selected examples, $Mn_4O_4(H_2O)_4^+$ and $Mn_4O_4(H_2O)_6^+$. The left column of Figure 3 shows the experimental IR-MPD spectrum of $Mn_4O_4(H_2O)_4^+$ (top) together with the calculated vibrational spectra of different isomers. The theoretically predicted minimum energy structure (4-a) is similar to structure 3-a in Figure 1 with an additional hydroxyl group resulting from the dissociation of the fourth water molecule. The first two isomers are 30 kJ mol^{-1} (4-b) and 37 kJ mol^{-1} (4-c) higher in energy. Both isomers show a similar structural motif of the cluster core as 4-a; however, they contain one and two intact water molecules, respectively. Isomeric structures comprising a distinct cuboidal Mn_4O_4 cluster core are even higher in energy (65 kJ mol^{-1} for 4-d and 91 kJ mol^{-1} for 4-e). Common to all the structures with molecularly adsorbed H_2O is that the intact water molecules bind by coordination of the O atom to a Mn atom and an H-bond to a neighboring OH group to form an H_3O_2 subunit.

To explore whether the observed spectra can be assigned to specific calculated structures, we make the following observations. The calculated vibrational spectrum for each isomer shows a number of features below 600 cm^{-1} in agreement with the broad band observed experimentally (labeled I in Figure 3, left column). The broad unstructured nature of this band makes it difficult to draw any firm conclusions. The bands labeled II and III between 650 cm^{-1} and 900 cm^{-1} are more diagnostic. The absence of any predicted band in this region appears to rule out isomer 4-e. Among the other isomers, the calculated spectral features of isomer 4-b are in most favorable agreement with bands II and III of the experimental spectrum.

The water bending mode spectral region (band IV) is a second diagnostic. The minimum energy isomer (4-a) contains only dissociated water and thus does not exhibit a mode in this region. In contrast, all other predicted isomers bind at least one intact H_2O molecule which is reflected by the appearance of an HOH bending mode. Experimentally, the mode is observed at 1624 cm^{-1}, in perfect agreement with the predicted mode for isomer 4-b at 1621 cm^{-1}. Interestingly isomer 4-b can be obtained by the removal of an intact H_2O molecule from the $Mn_4O_4(H_2O)_5^+$ isomer with −663 kJ mol^{-1} (Supporting Information, Figure S6); this process is portrayed in Figure 2 by the correlated depletion at 1621 cm^{-1} for $n=5$ with the enhancement in $n=4$. Isomer 4-c, with two intact water molecules, has two predicted water bending modes in this region, but the experiment shows no sign of a doublet depletion structure (since the loss of one water molecule

represents the only fragmentation channel observed after absorption of light in the HOH bending mode region, this would also be readily visible in the gain in $Mn_4O_4(H_2O)_3^+$ shown in Figure 2). Less intense predicted features in the calculated spectra of isomers containing intact water, between 1050 cm^{-1} and 1300 cm^{-1}, are not visible in the experiment; if present, these are obscured by a gain ($I/I_0 > 1$) since $Mn_4O_4(H_2O)_4^+$ appears to be a fragmentation product of a larger cluster complex in this frequency range.

Thus, among the first five lowest energy structures of $Mn_4O_4(H_2O)_4^+$, the calculated vibrational spectrum of isomer 4-b with an open cuboidal structure exhibits the most favorable agreement with the experimental IR-MPD spectrum. We cannot rule out explicitly the presence of the minimum energy isomer 4-a, which exhibits a similar structural motif, as it does not possess any diagnostic band that sets it off from other isomers. On the same grounds, we cannot rule out the presence of isomer 4-d with two activated water molecules either; the contribution from this isomer could be responsible for the observed (small) depletion centered around 1450 cm^{-1}. The coexistence of several isomers is not unlikely in the present experimental approach, in which the $Mn_4O_4(H_2O)_n^+$ complexes are formed under high-pressure conditions and quenched in the subsequent supersonic expansion. Thus, the stabilization of a higher energy isomer is possible as has been demonstrated previously for other systems.[8]

At the bottom of the left column in Figure 3, we show the calculated total vibrational density of states (vDOS) for isomer 4-b (red curve) as well as the projected vibrational density of states (pvDOS; green and blue curves). The difference between the red and green curve represents the contributions of H_2O and H_3O_2 units to the vibrational density of states, the difference between the green and blue curve represents the contributions of O atoms and OH groups, and the blue curve corresponds to the contributions of the Mn atoms. The pvDOS analysis (see the Supporting Information) allows for the assignment of three distinct regions: 1) vibrations at wavenumbers smaller than 600 cm^{-1} correspond to Mn-O-Mn motions of the cluster core; 2) vibrations in the region 600–1000 cm^{-1} can be assigned mainly to modes associated with vibrational displacements of OH subunits such as librations/rotations of the OH groups and Mn-OH stretch vibrations; librations of intact water molecules may also contribute in this region; 3) vibrations at wavenumbers larger than 1000 cm^{-1} typically arise from vibrational displacements of H_2O and H_3O_2 groups including the HOH bending motions in the proximity of 1600 cm^{-1}.

$Mn_4O_4(H_2O)_6^+$ is the smallest complex for which a complete cuboidal minimum energy structure has been predicted (6-a in Figure 1). The right column of Figure 3 shows the experimental IR-MPD spectrum (top panel) together with the calculated vibrational spectra of the minimum energy structure (6-a) and the first three higher-energy isomers (6-b to 6-d). Structures 6-a and 6-b (+32 kJ mol^{-1}) both contain a cuboidal $Mn_4O_4^+$ cluster core with fully hydroxylated μ_3-oxo bridges. Isomers 6-c and 6-d are 45 kJ mol^{-1} and 50 kJ mol^{-1} higher in energy, respectively, and have an open cube unit similar to the lowest energy isomers of $Mn_4O_4(H_2O)_4^+$ and $Mn_4O_4(H_2O)_5^+$. In 6-c, all oxo bridges are hydroxylated, whereas 6-d contains two non-hydroxylated bridges.

The calculated vibrational spectra of all isomers show numerous modes below 600 cm^{-1} as well as between 600 cm^{-1} and 850 cm^{-1} which are all in favorable agreement with the broad feature I and the signals II and III observed experimentally. Above 850 cm^{-1}, the calculated spectra exhibit few distinct signals while the experimental spectrum has another broad signal band (IV). Most interestingly, the experimental HOH bending mode (V) is found at 1619 cm^{-1}, which is in most favorable agreement with the corresponding modes of the cuboidal minimum energy structure 6-a at 1621 cm^{-1} and 1633 cm^{-1}. Owing to the spectral width of experimental band V, these two signals are not clearly distinguishable. For isomer 6-b two modes at 1560 cm^{-1} and 1625 cm^{-1} are predicted. While the latter mode may also be in agreement with the experimentally observed HOH bending mode, there is however no sign of the first more intense mode in the IR-MPD spectrum. In contrast, the HOH bending modes of isomer 6-c are blue-shifted to 1681 cm^{-1} and 1703 cm^{-1}, respectively, which is the edge of the detection range. Isomer 6-d has four intact H_2O and consequently four HOH bending modes: a red-shifted doublet at 1599 cm^{-1} and 1601 cm^{-1} and a blue-shifted doublet at 1643 cm^{-1} and 1658 cm^{-1}. The IR-MPD spectrum appears to be in most favorable agreement with the theoretically predicted cuboidal minimum energy structure 6-a, with likely contributions from higher-energy isomers, accessible under the non-equilibrium conditions prevailing in the supersonic expansion experiment; here we reiterate that the accuracy of the isomer-ordering has been verified with the inclusion of van der Waals interactions in the DFT calculations (see the Supporting Information).

The above assignment of the vibrational modes is further supported by the vDOS (red curve) and pvDOS (green and blue curves) for isomers 6-a and 6-c in Figure 3. Noteworthy is the difference of the contributions from the Mn atoms for a cuboidal and a more open cluster core structure illustrated by the blue curves (pvDOS projected on the Mn atoms).

Finally, the noted broadening of the experimentally observed spectral features in the case of $Mn_4O_4(H_2O)_6^+$ may be attributed not only to the presence of two structural isomers, but can also be a reflection of additional effects: reactivity experiments with isotopically labeled $H_2{}^{18}O$ have demonstrated the exchange of cluster ^{16}O with water ^{18}O atoms which also requires structural transformations of the $Mn_4O_4^+$ cluster core.[3b] Consequently, $Mn_4O_4(H_2O)_n^+$ are highly fluxional complexes, and broadening of the observed features by such dynamics is very likely. Interestingly, dynamical structural changes have also been emphasized for the natural OEC.[9] Such effects become of course more pronounced with increasing number of water molecules attached to the cluster.

In conclusion, first-principles simulations and IR-MPD vibrational spectroscopy give direct evidence that the splitting of the O–H bond of water through hydroxylation of Mn-O-Mn μ-oxo bridges is central to the interaction of water molecules with free $Mn_4O_4(H_2O)_n^+$ clusters. This reaction, which proceeds by a 1,3-hydrogen shift,[3b] occurs already for the first H_2O molecule interacting with the manganese oxide

cluster and continues for all subsequent water adsorption reactions until all available μ-oxo-bridges are hydroxylated. Further water molecules are bound molecularly with a preference for the formation of hydrogen-bridge-bound H_3O_2 units involving the hydroxylated μ-oxo-bridges.

Adsorbed water induces significant structural and dimensionality transformations. In $Mn_4O_4(H_2O)_n^+$ with $n \geq 3$ open-cuboidal-like structures emerge, and for $n \geq 6$ the $Mn_4O_4^+$ cluster core attains a closed cuboidal structure of comparable geometry to the active manganese-oxide-based center in the natural OEC of PSII. This is particularly interesting, since the natural cluster is additionally stabilized by carboxylate groups,[4b] and thus the nature of the ligands appears to be not crucial for the cluster geometry. This further supports our conclusion[3b] that free $Mn_4O_4(H_2O)_n^+$ complexes bring forth suitable model systems which are closely related to the biological OEC while being simple enough to provide molecular level insight into the interaction with water. Further steps in our hierarchical modelling approach will include the increase of the cluster size, the addition of Ca, and the distinct tailoring of the Mn oxidation states through the addition of appropriate ligands.

Acknowledgements

We gratefully acknowledge the Stichting voor Fundamenteel Onderzoek der Materie (FOM) for the support of the FELIX Laboratory. The research leading to these results has received funding from the European Community's Seventh Framework Programme (FP7/2007-2013) under grant agreement no. 312284. S.M.L. is grateful to the ESF Baden-Württemberg for a Margarete von Wrangell fellowship. R.N.B. was supported by grant No. FG05-86ER45234 from the Office of Basic Energy Sciences of the US Department of Energy (DOE) and U.L. by the Air Force Office for Scientific Research (AFOSR). D.M.K. acknowledges support from the Netherlands Organisation for Scientific Research (NWO) as part of the Dutch Astrochemistry Network. Computations were carried out at the Georgia Tech Center for Computational Materials Science.

Keywords: ab initio calculations · manganese oxide · oxygen evolving complex · vibrational spectroscopy · water splitting

How to cite: *Angew. Chem. Int. Ed.* **2015**, *54*, 15113–15117
Angew. Chem. **2015**, *127*, 15328–15332

[1] a) M. Yagi, M. Kaneko, *Chem. Rev.* **2001**, *101*, 21–35; b) S. Mukhopadhyay, S. K. Mandal, S. Bhaduri, W. H. Armstrong, *Chem. Rev.* **2004**, *104*, 3981–4026; c) R. Brimblecombe, G. F. Swiegers, G. C. Dismukes, L. Spiccia, *Angew. Chem. Int. Ed.* **2008**, *47*, 7335–7338; *Angew. Chem.* **2008**, *120*, 7445–7448; d) G. C. Dismukes, R. Brimblecombe, G. A. N. Felton, R. S. Pryadun, J. E. Sheats, L. Spiccia, G. F. Swiegers, *Acc. Chem. Res.* **2009**, *42*, 1935–1943; e) M. Wiechen, H.-M. Berends, P. Kurz, *Dalton Trans.* **2012**, *41*, 21–31; f) J. S. Kanady, E. Y. Tsui, M. W. Day, T. Agapie, *Science* **2011**, *333*, 733–736; g) J. S. Kanady, P.-H. Lin, K. L. Carsch, R. J. Nielsen, M. K. Takase, W. A. Goddard III, T. Agapie, *J. Am. Chem. Soc.* **2014**, *136*, 14373–14376; h) C. Zhang, C. Chen, H. Dong, J.-R. Shen, H. Dau, J. Zhao, *Science* **2015**, *348*, 690–693.

[2] M. M. Najafpour, T. Ehrenberg, M. Wiechen, P. Kurz, *Angew. Chem. Int. Ed.* **2010**, *49*, 2233–2237; *Angew. Chem.* **2010**, *122*, 2281–2285.

[3] a) S. M. Lang, I. Fleischer, T. M. Bernhardt, R. N. Barnett, U. Landman, *Nano Lett.* **2013**, *13*, 5549–5555; b) S. M. Lang, I. Fleischer, T. M. Bernhardt, R. N. Barnett, *J. Phys. Chem. C* **2015**, *119*, 10881–10887.

[4] a) Y. Umena, K. Kawakami, J.-R. Shen, N. Kamiya, *Nature* **2011**, *473*, 55–61; b) M. Suga, F. Akita, K. Hirata, G. Ueno, H. Murakami, Y. Nakajima, T. Shimizu, K. Yamashita, M. Yamamoto, H. Ago, J.-R. Shen, *Nature* **2015**, *517*, 99–103.

[5] A. Fujii, K. Mizuse, *Int. Rev. Phys. Chem.* **2013**, *32*, 266–307.

[6] a) S. M. Lang, T. M. Bernhardt, M. Krstić, V. Bonačić-Koutecký, *Phys. Chem. Chem. Phys.* **2014**, *16*, 26578–26583; b) S. Feyel, D. Schröder, H. Schwarz, *Eur. J. Inorg. Chem.* **2008**, 4961–4967; c) P. J. Roach, W. H. Woodward, A. W. Castleman Jr., A. C. Reber, S. N. Khanna, *Science* **2009**, *323*, 492–495; d) D. W. Rothgeb, E. Hossain, J. E. Mann, C. C. Jarrold, *J. Chem. Phys.* **2010**, *132*, 064302; e) J.-B. Ma, Y.-X. Zhao, S.-G. He, X.-L. Ding, *J. Phys. Chem. A* **2012**, *116*, 2049–2054; f) M. Arakawa, K. Kohara, T. Ito, A. Terasaki, *Eur. Phys. J. D* **2013**, *67*, 80; g) T. D. Jaeger, A. Fielicke, G. von Helden, G. Meijer, M. A. Duncan, *Chem. Phys. Lett.* **2004**, *392*, 409–414.

[7] R. N. Barnett, U. Landman, *Phys. Rev. B* **1993**, *48*, 2081–2097.

[8] a) C. Kerpal, D. J. Harding, D. M. Rayner, A. Fielicke, *J. Phys. Chem. A* **2013**, *117*, 8230–8237; b) A. Fielicke, R. Mitrić, G. Meijer, V. Bonačić-Koutecký, G. von Helden, *J. Am. Chem. Soc.* **2003**, *125*, 15716–15717.

[9] a) M. Haumann, C. Müller, P. Liebisch, L. Iuzzolino, J. Dittmer, M. Garbolle, T. Neisius, W. Meyer-Klaucke, H. Dau, *Biochemistry* **2005**, *44*, 1894–1908; b) A. Klauss, T. Sikora, B. Süss, H. Dau, *Biochem. Biophys. Acta Bioenergetics* **2012**, *1817*, 1196–1207.

Received: July 9, 2015
Revised: September 24, 2015
Published online: October 23, 2015

